Structural and magnetic instabilities of two-dimensional quantum spin systems

Carsten H. Aits,[1] Ute Löw,[1] Andreas Klümper,[2] and Werner Weber[3]
[1]*Institut für Theoretische Physik, Universität zu Köln, Zülpicherstrasse 77, 50937 Köln, Germany*
[2]*Universität Wuppertal, Gaussstrasse 20, 42097 Wuppertal, Germany*
[3]*Institut für Physik, Universität Dortmund, Otto Hahn-Strasse 4, D-44221 Dortmund, Germany*
(Received 23 March 2006; published 20 July 2006)

We present a study of the magnetic order and the structural stability of two-dimensional quantum spin systems in the presence of spin-lattice couplings. For a square lattice it is demonstrated that the plaquette deformation yields the strongest gain in magnetic energy. The analysis of the dimer-dimer response function further shows that lattice distortions may generally coexist with magnetic long-range order, in contrast to the one-dimensional case. Similarly, the coupling to Einstein phonons is found to reduce, but not to eliminate, the staggered magnetic moment. In addition, we consider the renormalization of the square lattice phonon spectrum due to spin-phonon coupling in the adiabatic approximation. Toward low temperatures, significant softening mainly of zone boundary phonons is found, especially around the $(\pi,0)$ point of the Brillouin zone. This result is compatible with the tendency to plaquette formation in the static limit. We also point out the importance of a "magnetic pressure" on the lattice due to spin-phonon coupling. At low temperatures, this results in a tendency toward shear instabilities of the lattice.

DOI: 10.1103/PhysRevB.74.014425 PACS number(s): 75.10.Jm, 75.50.Ee, 03.65.−w, 73.43.Nq

I. INTRODUCTION

Considering the immense wealth of materials newly synthesized or found in nature with low-dimensional magnetic structure, one finds that the simple Heisenberg Hamiltonian, widely accepted as the paradigm of quantum magnets,[1,2] is often complicated by further interactions. Many compounds thus show ground states and phases, different from the generic long-range magnetic order of Heisenberg systems.

In this paper, we study the coupling of the magnetic degrees of freedom to lattice vibrations as a prominent example of an interaction "beyond the Heisenberg Hamiltonian." This coupling, often referred to as "spin-phonon" interaction, is generic to *all* magnetic materials and thus the problem of to what extent the magnetic structure is changed by its presence concerns all low-dimensional magnetic compounds.

Though spin-phonon couplings are ubiquitous in nature, the possibilities of treating them with some theoretical rigor are limited. The main reason is that magnetic and phononic excitation energies are not well separated. In contrast, for electron phonon coupling we can dwell on the fact that the bulk of the electronic excitations lies much higher in energy than the phonon modes. This allows us, in general, to use the adiabatic approximation when calculating the renormalization of phonon frequencies due to electron-phonon coupling. For spin-phonon coupling, however, this concept cannot be applied, in general.

One approach quite often used is to include local, Einstein-type phonons as quantum-mechanical objects. This model may be applied for certain vibrations of ligand atoms around the magnetic ions, but it is not very realistic as it violates the infinitesimal translational invariance of the lattice.

For relatively low-lying acoustic phonons, which are dominated by the heavy magnetic ions, the response of the spin system may be treated in an adiabatic approximation. In one dimension, the paper of Cross and Fisher[3] has treated the spin-phonon coupling along such lines. In higher dimensions, no study of spin-phonon coupling in the adiabatic limit has been presented as yet.

In addition, any effect of the magnetic pressure on the phonon vibrations has been ignored so far. The magnetic energy of a square lattice of spins with first-nearest-neighbor (1NN) antiferromagnetic coupling $J(a)$ is given as $E_m = U(T)J(a)$, which is typically of the order -0.1 eV per atom. We may compare this magnetic energy with the energy $E_{\mathrm{Mad}}=-\alpha_M(e^2/a)$ of a cubic lattice of positive and negative elementary charges where the Madelung constant α_M is of order of unity. For rock salt we find, e.g., $E_{\mathrm{Mad}}\approx -8$ eV. However, the pressure $\partial U/\partial V$ for the electrostatic system is ≈ 0.1 eV/Å^3, while ≈ 0.015 eV/Å^3 for the magnetic system. Although there is a factor of ≈ 100 difference in the binding energies, the magnetic pressure is only a factor 10 smaller compared to the pressure of the electrostatic system. The main reason for the relatively large magnetic pressure is the large spin phonon coupling caused by the strong distance dependence of the superexchange $J(a)$, which cannot be neglected in describing realistic quantum spin systems.

As an important special case, we also discuss the limit of very strong spin phonon coupling, which leads to a dimerization of the lattice. Typically, the response of the ground-state energy of a two-dimensional magnetic system to dimerization is of second order and thus much weaker than in the one-dimensional case. Two-dimensional models with dimerization are thus essentially different compared to their one-dimensional analogues; in particular, in two dimensions dimerization does not necessarily lead to a breakdown of magnetic long-range order. Also the dimerization pattern, which leads to the lowest ground state, is not clear in two dimensions.

This paper is organized as follows. In Sec. II A, we study statically dimerized models; in particular, we determine the optimal dimerization pattern in two dimensions. Section II B is devoted to Einstein phonons coupled to two-dimensional

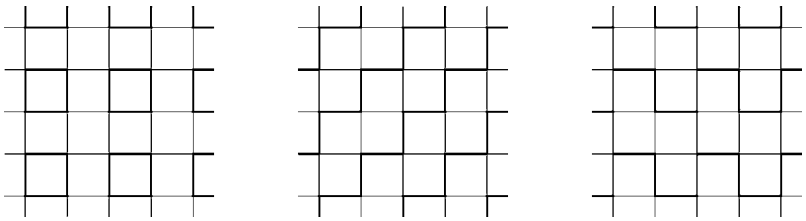

FIG. 1. Plaquette, stair, and meander configurations as possible dimerization patterns with minimal unit cell in two dimensions.

spin systems. In Sec. III, we calculate explicitly the phonon spectrum and study structural instabilities driven by the spin-phonon coupling including the effect of the "magnetic pressure."

II. STATICALLY DIMERIZED MODELS AND EINSTEIN PHONONS

A. The dimerized model with optimal deformation patterns

To approach the problem, we assume in the first place that in two dimensions similar to one-dimensional systems the spin lattice interactions lead to a transition to a dimerized state, i.e., to a pattern of strong and weak bonds, and we address the problem of the two-dimensional correspondence of a dimerized chain.

Stair, plaquette, and meander configurations (see Fig. 1) are obvious choices for such models, which have been discussed controversially in the literature.[4–6]

Here we show by a straightforward Monte Carlo calculation [7] that the plaquette models have lowest energy. This is convincingly demonstrated in Fig. 2, where the extrapolated energies of the three configurations are shown.

It is not clear, however, whether configurations with larger unit cells or even disordered systems can still have lower energies. To clarify this point, we analyze Hamiltonians of the type

$$H(\delta) = 2J\sum_{ij}\left[(1+A_{ij}\delta)\vec{S}_{ij}\vec{S}_{i+1,j} + (1+B_{ij}\delta)\vec{S}_{ij}\vec{S}_{i,j+1}\right] \quad (1)$$

for all possible $A_{ij}, B_{ij} = \pm 1$, with an equal number of strong and weak bonds, $M = \Sigma_{i,j}(A_{ij}+B_{ij}) = 0$. Here A_{ij} and B_{ij} specify the pattern and δ gives the strength of the deformation. This Hamiltonian of course includes the configurations of Fig. 1 as special cases.

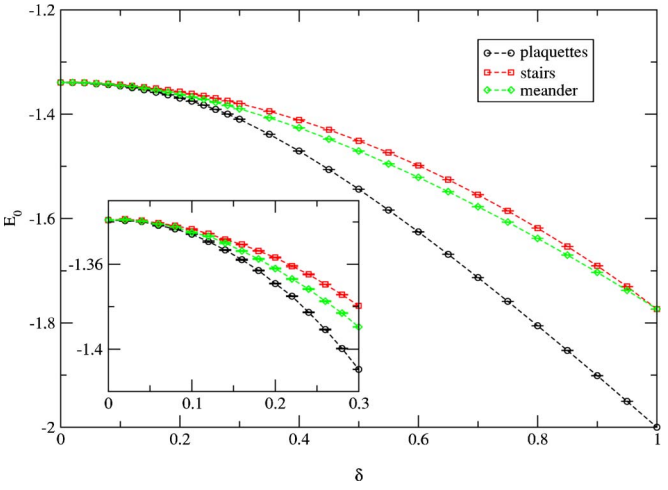

FIG. 2. (Color online) Extrapolated ground-state energies for the three dimerization patterns shown in Fig. 1.

This more general study stems from an expansion of the free energy of the system Eq. (1) in δ,

$$F(\delta,T) = F(0,T) + \frac{1}{2}a(T)\delta^2 + \frac{1}{24}b(T)\delta^4 + O(\delta^6). \quad (2)$$

Writing down $a(T)$ explicitly, we observe that it can be viewed as a Hamiltonian of a two-layer Ising model with Ising spins A_{ij} and B_{ij},

$$a(T) = \left.\frac{\partial^2 F}{\partial \delta^2}\right|_{\delta=0} = 4J^2 \sum_{ijd_1d_2} \{K^{xx}(d_1,d_2)A_{ij}A_{i+d_1,j+d_2} + K^{yy}(d_1,d_2)B_{ij}B_{i+d_1,j+d_2} + K^{xy}(d_1,d_2)A_{ij}B_{i+d_1,j+d_2} + K^{yx}(d_1,d_2)B_{ij}A_{i+d_1,j+d_2}\}, \quad (3)$$

where the couplings of the Ising model are given by dynamic dimer correlations,

$$K^{qr}(d_1,d_2) = -\int_0^\beta d\tau \langle D^q_{00}(0) D^r_{d_1d_2}(\tau)\rangle, \quad (4)$$

evaluated in the two-dimensional Heisenberg model, i.e., for $\delta = 0$. Here q and r are either x or y corresponding to dimer operators $D^x_{ij} = \vec{S}_{ij}\vec{S}_{i+1,j}$ or $D^y_{ij} = \vec{S}_{ij}\vec{S}_{i,j+1}$. This means the quantum nature of the model is incorporated in the long-ranged Ising couplings, which depend on the Euclidean dynamical dimer correlation functions of the isotropic Heisenberg model. This "perturbative approach" is somewhat restrictive, but we are interested in the phenomenologically relevant small dimerizations. Also, with some more numerical effort, quadruple and higher correlations could be studied and for large dimerizations the problem becomes rather trivial, since it is reduced to one-dimensional Heisenberg chains whose properties are well known.

The dimer correlations Eq. (4) of the Heisenberg model (as well as the data shown in Fig. 2) were evaluated using a quantum Monte Carlo (QMC) loop algorithm,[8,9] based on a path integral representation of the partition function.[10] Applying the loop algorithm, autocorrelation effects play a minor role due to global spin updates, and expectation values of diagonal and off-diagonal operators are calculated efficiently within the framework of improved estimators.[11,13] Further, by taking the continuous time version of the algorithm,[12] finite-size effects in the Trotter direction are avoided.

With the dimer correlations Eq. (4) as coupling constants of the Ising model, we performed a standard classical Monte Carlo simulation together with some cooling procedure.[14,15]

This analysis gives clear evidence for crossing stripe patterns in the plane of the A and B spins as the ground state of the Ising model.[16] This amounts to a plaquette structure as the lowest pattern of the model Eq. (1).

In contrast to the one-dimensional case where $a(T)$ is divergent[17] when T approaches zero, $a(T)$ stays finite in two dimensions, which *a posteriori* justifies our ansatz.

A crucial point that further distinguishes the one-dimensional case from the two-dimensional is the presence of *both* long-range magnetic order and a finite dimerization in the two-dimensional plaquette model, whereas in one dimension any finite δ leads to a spin liquid ground state with a gapped excitation spectrum.

For static phonons we definitely observe a breakdown of long-range magnetic order for sufficiently strong deformation δ. The critical value δ_c takes rather large and in general different values for different patterns. For the stair configuration δ_c takes its maximal value 1, at which the system decouples into one-dimensional subsystems. For the plaquette configuration, δ_c is considerably smaller than 1 (in the cluster series expansion approach $\delta_c \approx 0.3$), [18,19] while we determined from our data $\delta_c = 0.291(3)$.

B. The effect of Einstein phonons in two dimensions

To study the impact of a spin-phonon coupling on the magnetic long-range order, we next consider a two-dimensional (2D) model coupled to Einstein phonons. Although the model is not realistic in many respects, it has still attracted a lot of attention, and for the physics of its one-dimensional form, a fairly clear picture has emerged by now. In particular, it is well known that the quasi-long-range order, leading to a logarithmic divergence in the structure factor at $q=\pi$, is destroyed by a relatively small spin-phonon coupling. This brings about the problem of to what extent the strong long-range order of 2D systems is influenced in the presence of Einstein phonons. To answer this, we calculate the expectation value of the staggered magnetization operator,

$$\vec{M}_{\mathrm{st}} = \sum_{x,y} (-1)^{(x+y)} \vec{S}_{x,y}, \tag{5}$$

which is a measure of Néel order in the ground state. We adopt the common procedure (see Refs. 20 and 21) and compute the expectation value of $\vec{M}_{st}^2$,

$$M^2 := \frac{1}{N^4} \langle 0 | \vec{M}_{\mathrm{st}}^2 | 0 \rangle, \tag{6}$$

for the full quantum Hamiltonian of spins $\vec{S}_{ij}$ at sites ij coupled to Einstein phonons b_{ij}^x and b_{ij}^y by a spin-phonon coupling g,

$$\begin{aligned} H = {} & 2J \sum_{i,j=1}^{N} \vec{S}_{ij} \vec{S}_{i+1,j} (1 + g[b_{ij}^x + b_{ij}^{x\dagger}]) \\ & + 2J \sum_{i,j=1}^{N} \vec{S}_{ij} \vec{S}_{i,j+1} (1 + g[b_{ij}^y + b_{ij}^{y\dagger}]) \\ & + \omega \sum_{i,j=1}^{N} (b_{ij}^{x\dagger} b_{ij}^x + b_{ij}^{y\dagger} b_{ij}^y). \end{aligned} \tag{7}$$

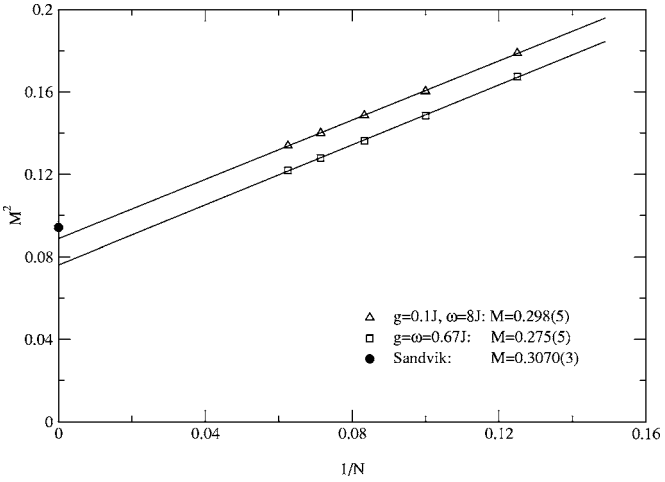

FIG. 3. Staggered magnetization M^2 for the model Eq. (7) as a function of linear lattice size. The black circle is the value for the Heisenberg model from Ref. 21.

To study this Hamiltonian, we employ a Monte Carlo method, which was developed in Refs. 22 and 23. It allows us to treat up to 50 phonons per site, and is practically free of truncation errors. As expected, we find Heisenberg-like behavior in the case of small spin-phonon couplings g and large values of the phonon frequency ω. It is remarkable, however, that for parameters for which in the one-dimensional model[22,24] one finds clear evidence for a finite correlation length at $T=0$, the staggered magnetization is again nonzero, and its extrapolated value is only about 10% reduced compared to the two-dimensional Heisenberg model. Also, M^2 displays a dominant $1/N$ finite-size behavior[21,25,26] derived from the nonlinear sigma model description of the Heisenberg model (see Fig. 3).

Though we cannot exclude a breakdown of long-range order by studying even larger spin-phonon couplings or different, maybe more elaborate, coupling mechanisms, we find that a realistic coupling strength comparable to the ones found in one-dimensional magnetic materials will *not* lead to a breakdown of long-range order. So, the new feature we expect in two dimensions is the possibility of a structural phase transition driven by spin-phonon interactions without breakdown of long-range order.

III. STRUCTURAL PHASE TRANSITIONS

To investigate the structural phase transition also from a phenomenological point of view, we consider the following two-dimensional Heisenberg Hamiltonian coupled to classical phonons,

$$H = 2J \sum_{l,m} \frac{1}{2} [1 + \lambda (\vec{u}_l - \vec{u}_m) \hat{R}_{lm}] \vec{S}_l \vec{S}_m, \tag{8}$$

with $\vec{S}_l$ a spin-$\frac{1}{2}$ operator at position $\vec{r}_l$, $\vec{R}_{lm} = \vec{R}_l - \vec{R}_m$ the distance vector between sites l and m at equilibrium, $\hat{R}_{lm} = \vec{R}_{lm} / |\vec{R}_l - \vec{R}_m|$, and $\vec{u}_l = \vec{r}_l + \vec{R}_l$ the displacement vector of the (l)th spin from equilibrium. The summation in Eq. (8) runs

over nearest neighbors l and m. [Note that to simplify the notation, we abbreviate from now on the two spatial indices (i,j) used, e.g., in Eq. (1) by only one index and continue to use the coupling strength $2J$ per bond.]

The total Hamiltonian consists of a sum of the Hamiltonian H for all layers plus the phonon contributions Φ, which we assume to be derivable from a simple model with central force potentials $\Phi_1(|\vec{r}_l-\vec{r}_m|)$ and $\Phi_2(|\vec{r}_l-\vec{r}_m|)$, which depend on the nearest-neighbor and the next-nearest-neighbor (diagonal) distances between the ions,

$$\Phi = \frac{1}{2}\sum_{l\neq m}[\Phi_1(|\vec{r}_l-\vec{r}_m|)+\Phi_2(|\vec{r}_l-\vec{r}_m|)]. \tag{9}$$

Thus in equilibrium the total energy $E(a)$ per site is given by

$$E(a) = 2\Phi_1(a) + 2\Phi_2(\sqrt{2}a) + 2U(T)J(a), \tag{10}$$

where $U(T)<0$ is the internal energy per site of the Heisenberg model with $J=1$ and a is the lattice constant. The magnetic energy $U(T)J(a)$ has the tendency to compress the lattice as the superexchange coupling $J(a)$, which may be derived from a Hubbard-type model, increases with decreasing lattice constant a. When we treat this magnetic pressure as an external pressure acting on the lattice, the equilibrium condition $dE/da=0$ yields

$$2B + 4B' + \frac{2}{a}J\lambda U(T) = 0. \tag{11}$$

Here $\lambda = d\ln J(a)/da$ is again the spin-phonon coupling, and following [27] the force constants B and B' are defined as

$$B^{(i)} := \frac{1}{R_{lm}}\frac{d\Phi^{(i)}}{dR_{lm}} \tag{12}$$

with $R_{lm}=|\vec{R}_l-\vec{R}_m|$ the equilibrium separation for either first- or second-neighbor pairs. The full force constant matrix $\Phi^{(i)}_{\alpha\beta}$ is given by [27]

$$\Phi^{(i)}_{\alpha\beta} = A^{(i)}\hat{R}^{\alpha}_{lm}\hat{R}^{\beta}_{lm} + B^{(i)}(\delta^{\alpha\beta}-\hat{R}^{\alpha}_{lm}\hat{R}^{\beta}_{lm}) \tag{13}$$

with

$$A^{(i)} = \frac{d^2}{dR^2_{lm}}\Phi^{(i)}(R_{lm}). \tag{14}$$

In any reasonable model of 1NN and 2NN force constants A,B and A',B',

$$|B|<A \quad \text{and} \quad |B'|<A' \tag{15}$$

can be expected from the requirement that longitudinal phonon frequencies are in general considerably larger than transverse ones. One should keep in mind that our model for a square lattice of magnetic ions ignores additional forces acting via the closed-shell ligands, which may also contribute to the equilibrium condition Eq. (11), so that without the magnetic pressure, $B+2B'$ could be chosen positive. When, however, the magnetic pressure is turned on, by lowering T, $B+2B'$ will become negative (or strongly reduced), which will affect, in particular, the stability of the lattice against shear.

The elements of the dynamical matrix $G_0^{\alpha\beta}(\vec{q})$ of the "bare" phonons are given by

$$G_0^{xx}(\vec{q}) = 2A(1-\cos x) + 2B(1-\cos y) + 2(A'+B')(1-\cos x\cos y),$$

$$G_0^{yy}(\vec{q}) = 2A(1-\cos y) + 2B(1-\cos x) + 2(A'+B')(1-\cos x\cos y),$$

$$G_0^{xy}(\vec{q}) = 2(A'-B')\sin x\sin y \tag{16}$$

with $x=q_xa$ and $y=q_ya$.

We find the following phonon-dispersion relations for longitudinal and transverse modes. For $\vec{q}=(x,0)$,

$$m\omega_L^2(\vec{q}) = 2(A+A'+B')(1-\cos x), \tag{17}$$

$$m\omega_T^2(\vec{q}) = 2(B+A'+B')(1-\cos x). \tag{18}$$

For $\vec{q}=(x,x)$,

$$m\omega_L^2(\vec{q}) = 2(A+B)(1-\cos x) + 4A'\sin^2 x, \tag{19}$$

$$m\omega_T^2(\vec{q}) = 2(A+B)(1-\cos x) + 4B'\sin^2 x. \tag{20}$$

At long wavelength, the transverse frequencies are given as

$$m\omega_T^2(x,0) = [(B+2B')+A'-B']x^2, \tag{21}$$

$$m\omega_T^2(x,x) = [2(B+2B')+A-B]x^2. \tag{22}$$

In addition to the magnetic pressure, which is first order in λ, the spin-phonon coupling renormalizes the "bare" phonon frequencies similar to the renormalization due to electron-phonon coupling.

Similar to the analysis described in the first part of the paper, we again expand the free energy of the system Eq. (9) in terms of the lattice displacement and find an expression that is similar to Eq. (3). However, here the A_{ij} of Eq. (3) are replaced by $u^x_{i+1,j}-u^x_{ij}$ and the B_{ij} by $u^y_{i,j+1}-u^y_{ij}$. That is compared to Eq. (3) in which the classical displacements are no longer Ising variables but take continuous values. Thus to second order in the spin-phonon coupling we find for the dynamical matrix

$$G(\vec{q}) = G_0(\vec{q}) - \lambda^2 g(\vec{q}), \tag{23}$$

where the entries of the spin-phonon contribution

$$g^{xx} = 2(1-\cos x)\tilde{K}^{xx}(x,y),$$

$$g^{yy} = 2(1-\cos y)\tilde{K}^{yy}(x,y),$$

$$g^{xy} = g^{yx} = \tfrac{1}{2}(1-e^{ix})(1-e^{-iy})\tilde{K}^{xy}(x,y) + \text{c . c.} \tag{24}$$

involve the Fourier transforms $\tilde{K}^{qr}(x,y)$ of the dimer-dimer correlations Eq. (4). Note that the matrix g is real and symmetric, and from the symmetries of the dimer correlations follows $\tilde{K}^{xy}(\pi,\pi)=0$.

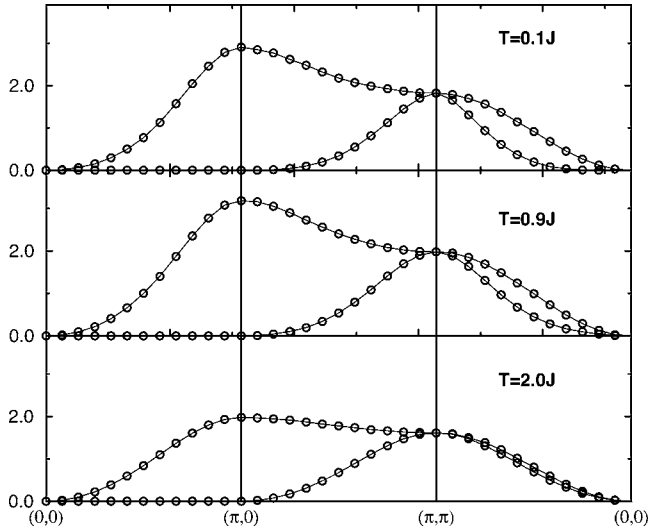

FIG. 4. Eigenspectra $\omega_{1,2}^2$ of the matrix g for $T/J=0.1$, $T/J=0.9$, and $T/J=2.0$ along a triangular path in $\vec{q}$ space.

Typical eigenvalues for the spin-phonon coupling matrix $g(x,y)$ along the symmetry lines of the square lattice are shown in Fig. 4. Several features are noteworthy.

(i) There is a considerable T dependence not only concerning the magnitude of the renormalization, but also the q dependence.

(ii) There is a maximum of the renormalization around $T/J=1$.

(iii) Along $(x,0)$ there is no renormalization of the transverse branch, similar to the absence of the electron-phonon coupling for transverse modes in a nearly-free-electron model.

(iv) At small T, a significant splitting of the eigenvalues along (x,x) evolves, indicative of an increase of $\tilde{K}^{xy}$ at low T.

(v) Also, the renormalization of the longitudinal branch along $(x,0)$ shows an increase of the effective 3NN force constant toward low T.

Points (iv) and (v) indicate that the effective forces between the atoms transmitted via the spin system become longer ranged at low T.

The phonon renormalization due to spin-phonon coupling may lead to significant softening and even to lattice instabilities.

The magnetic pressure effect lowers specific transverse phonon modes at long wavelengths, i.e., it destabilizes the lattice against certain shear deformations. This can be seen in Fig. 5, where the undisturbed spectrum of a square lattice (zeroth order in λ) which follows from Eq. (16) by setting $B=B'=0$ is shown together with the spectra including the external pressure and the second-order contribution. Here the equilibrium condition Eq. (11) is a strong constraint on the system and the shear instability dominates the phonon renormalization.

We should keep in mind, however, that realistic planar quantum antiferromagnets usually are ternary or even quaternary oxides and that the equilibrium condition of the lattice may be dominated by ligand contributions, not included in Eq. (11). As a consequence, we may ignore the magnetic pressure effect and consider solely the phonon renormalization due to the second-order effect. Here primarily zone boundary phonons are lowered, as may be seen from Fig. 6. For the calculation we have chosen typical values for the model force constants, which approximately reproduce the acoustic phonon modes of typical cubic oxides with rock salt structure[28] such as MgO or BaO.

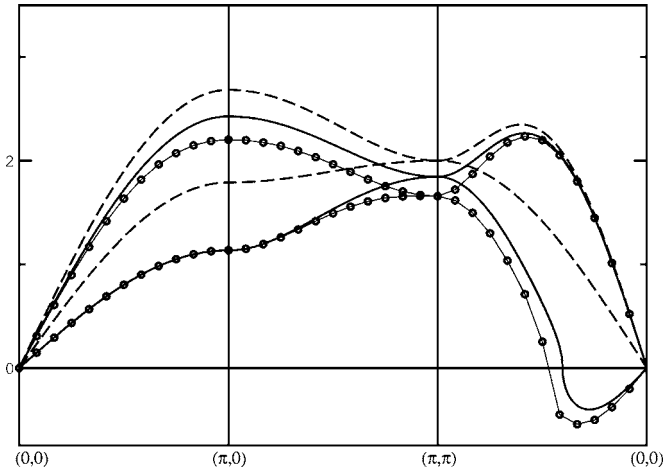

FIG. 5. Eigenspectra $\omega_{1,2}$ in zeroth (dashed line), first (solid line) and second order (circles) along a triangular path in $\vec{q}$-space for spin-phonon coupling $\lambda=-0.6$, $A'/A=0.8$, $B/J=-0.075$, $B'/J=-0.163$ and $T/J=0.1$. Note, that in the region of instability with $\omega_{1,2}^2<0$ we plot $-\sqrt{-\omega_{1,2}}$.

For a wide variety of A'/A ratios, we find that the softening is strongest near $(\pi,0)$; only for somewhat pathological choices of A,A',B,B' such as $A'-B'\approx 0$, $A'+B'\gg A$ do we find that the (π,π) frequency goes unstable first. The $(\pi,0)$ instability would lead to plaquette-like distortions, while the (π,π) instability would yield staircase distortions.

This means that our results from spin-phonon coupling agree with the observation discussed above, that the

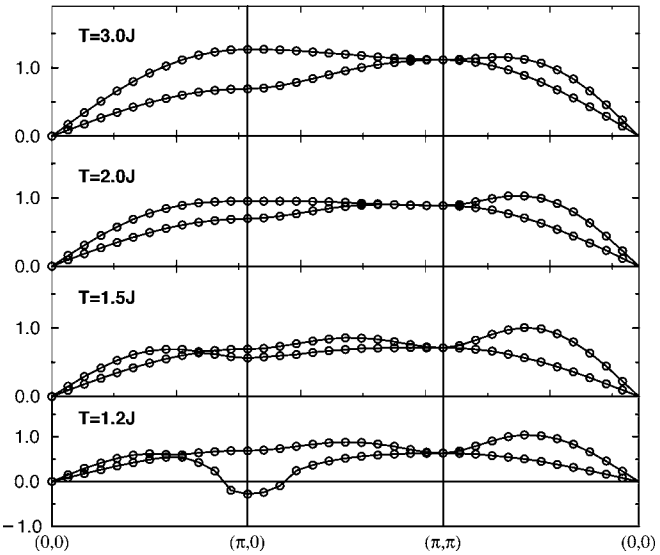

FIG. 6. Energies $\omega_{1,2}$ of the matrix G for $B=B'=0$. Again for $\omega_{1,2}^2<0$ we plot $-\sqrt{-\omega_{1,2}}$.

plaquette is the energetically most favorable dimerization pattern.

IV. SUMMARY

In this paper we have studied magnetic and structural instabilities of two-dimensional quantum antiferromagnets. Of the various dimerization patterns, the energetically most favorable one at $T=0$ is the plaquette order. It was also shown that the various dimerisation patterns do not necessarily lead to a breakdown of long-range magnetic order. In contrast to one dimension, the coupling to Einstein phonons is found to reduce, but not to destroy, the staggered magnetic moment.

The tendency to form dimerization patterns at sufficiently large spin-phonon coupling is also reflected in the large renormalization of specific phonon frequencies, in particular near $(\pi,0)$ and (π,π). Our results indicate that again, plaquette formations are the most favorable structural distortions.

In this paper, we also point out the importance of a "magnetic pressure" on the lattice caused by the relatively large spin-phonon coupling. This pressure effect builds up with decreasing T and may lead to a significant decrease, if not instability of specific shear elastic constants. Presently we have treated the magnetic pressure as an external one. In principle, it can also be included into the calculation of phonon frequency renormalization, e.g., by carrying out so called frozen phonon calculations, which is the ultimate form of the adiabatic approximation.

We finally remark that, wherever in the Brillouin zone there occur renormalization effects due to spin-phonon coupling, a significant increase of the phonon linewidth is also expected.

ACKNOWLEDGMENTS

We would like to thank D. Khomskii, E. Müller-Hartmann, and J. Sirker for useful discussions. This work was supported by the DFG through Grant No. SFB 608. Part of the simulations were carried out on the ZAM Höchstleistungsrechner Jülich.

[1] W. Heisenberg, Z. Phys. **49**, 619 (1928).
[2] H. A. Bethe, Z. Phys. **71**, 205 (1931).
[3] M. C. Cross and D. S. Fisher, Phys. Rev. B **19**, 402 (1979).
[4] S. Tang and J. E. Hirsch, Phys. Rev. B **37**, 9546 (1988).
[5] J. Sirker, A. Klümper, and K. Hamacher, Phys. Rev. B **65**, 134409 (2002).
[6] P. Sengupta, cond-mat/0307746 (unpublished).
[7] Note that the error due to finite temperatures is of the order of T^3, i.e., smaller than 6.0×10^{-5}. Therefore, within the statistical error, we can safely identify $U(T/J=0.04)$ with the ground-state energy.
[8] H. G. Evertz, G. Lana, and M. Marcu, Phys. Rev. Lett. **70**, 875 (1993).
[9] H. G. Evertz, in *Numerical Methods for Lattice Quantum Many-Body Problems*, edited by D. J. Scalapino (Addison Weasly, Reading, MA, 2001).
[10] M. Suzuki, S. Miyashita, and A. Kuroda, Prog. Theor. Phys. **58**, 1377 (1977).
[11] R. Brower, S. Chandrasekharan, and U.-J. Wiese, Physica A **261**, 520 (1998).
[12] B. B. Beard and U.-J. Wiese, Phys. Rev. Lett. **77**, 5130 (1996).
[13] J. V. Alvarez and C. Gros, Eur. Phys. J. B **15**, 641 (2000).
[14] U. Löw, V.-J. Emery, K. Fabricius, and S. A. Kivelson, Phys. Rev. Lett. **72**, 1918 (1994).
[15] D. L. Khomskii and U. Löw, Phys. Rev. B **69**, 184401 (2004).
[16] Note that the coupling of the Ising model depends on the temperature $T=1/\beta$ of the model Eq. (1). We need to find the ground state of the Ising model for every T (though we are mostly interested in low T). The temperature used in the Monte Carlo simulation of the Ising model is an auxiliary variable.
[17] A. Klümper, R. Raupach, and F. Schönfeld, Phys. Rev. B **59**, 3612 (1999).
[18] A. Koga, S. Kumada, and H. Kawakami, J. Phys. Soc. Jpn. **68**, 642 (1999).
[19] A. Voigt, Comput. Phys. Commun. **146**, 125 (2002).
[20] T. Barnes, Int. J. Mod. Phys. C **2**, 659 (1991).
[21] A. W. Sandvik, Phys. Rev. B **56**, 11678 (1997).
[22] R. W. Kühne and U. Löw, Phys. Rev. B **60**, 12125 (1999).
[23] C. H. Aits and U. Löw, Phys. Rev. B **68**, 184416 (2003).
[24] C. Raas, U. Löw, G. S. Uhrig, and R. W. Kühne, Phys. Rev. B **65**, 144438 (2002).
[25] S. Chakravarty and B. I. Halperin, and D. R. Nelson, Phys. Rev. B **39**, 2344 (1989).
[26] P. Hasenfratz and F. Niedermayer, Phys. Lett. B **268**, 231 (1991).
[27] A. A. Maradudin, E. W. Montroll, G. H. Weiss, and I. P. Ipatova, *Theory of Lattice Dynamics in the Harmonic Approximation* (Academic Press, New York, 1971).
[28] H. Bilz und W. Kress, *Phonon Dispersion Relations in Insulators*, Springer Series in Solid-State Sciences Vol. 10 (Springer-Verlag, Berlin, 1979).